Competition between commensurate and incommensurate phases in rare-earth systems: Effects on H-T magnetic phase diagrams

D. Gignoux and D. Schmitt
Laboratoire de Magnétisme Louis Néel, Centre National de la Recherche Scientifique, Boite Postale 166, 38042 Grenoble Cédex 9, France
(Received 16 February 1993; revised manuscript received 12 July 1993)

Some features common to many rare-earth intermetallic compounds with complex magnetic phase diagrams are explained using a realistic mean-field model, which takes into account the periodic-exchange-field and crystal-field effects which favor an easy magnetization axis, i.e.: (i) the change of an incommensurate or long-period commensurate structure near T_N toward a simple commensurate one at low temperature, with and without intermediate structures of intermediate propagation vectors; (ii) the low-temperature metamagnetic process during which the high-temperature propagation vector(s) tend to be recovered; (iii) the trend for the propagation vectors to lock onto commensurate values, except near T_N. Exchange interactions alone are enough to account for these properties, the exact boundaries of the magnetic phase diagram being determined by the real variation of $J(\mathbf{q})$ and crystal-field effects.

I. INTRODUCTION

Modulated systems with a period incommensurate with the basic lattice are not unusual in condensed-matter physics. The origin of such structures is the presence of competing interactions which can involve either the lattice, the conduction electrons, or the magnetic moments and manifest themselves in domains as different as linear atomic chains, incommensurate lattice distortion, ferroelectric substances, charge or spin density waves, and modulated magnetic structures.[1] In this latter case, the involved competing interactions are the long-range Ruderman-Kittel-Kasuya-Yosida (RKKY)–type exchange coupling, mediated from one magnetic ion to another through the conduction electrons. The oscillatory character of this coupling leads to antagonistic interionic interactions which often produce frustrated systems and hence incommensurate (helical or amplitude modulated) magnetic structures. This is particularly common in rare-earth intermetallic compounds where a considerable number of such structures has been discovered in the last two decades.[2]

The existence of incommensurate or long-period (high-order) commensurate magnetic structures leads to particularly interesting properties as a function of the temperature and/or the magnetic field. Indeed, the compounds in which such an incommensurate magnetic phase occurs at their ordering temperature T_N very often exhibit one or several *transitions* at lower temperatures toward other, generally simpler, magnetic phases with a different periodicity, i.e., where the period is shorter. Furthermore, in these systems, at low temperature, a *resurgence* of the incommensurability is frequently observed as soon as a magnetic field is applied, through one or several successive transitions (multistep behavior) until the induced ferromagnetic state is recovered. This behavior leads to complex magnetic H-T phase diagrams exhibiting several intermediate magnetic structures.[3] The role of the magnetocrystalline anisotropy is obviously fundamental in these systems by imposing, in particular, a preferential direction for the magnetic moments (axial anisotropy, modulated collinear structure) or by allowing the moments to be free to rotate within a given plane (planar anisotropy, helical structure).

Among the most recent phenomenological theories on the complex phase diagrams of magnetic systems with frustrated interactions one can cite the approaches of Bak and von Boehm,[4] Fisher and Selke,[5] and Selke and Duxbury[6] which are all similar. In a simple Ising model with exchange interactions between first (J_1) and second (J_2) nearest ferromagnetic planes [axial next-nearest-neighbor Ising (ANNNI) model], they have determined the possible spin arrangements in the space $(-J_1/J_2, T)$. Whereas long-period commensurate or incommensurate structures are stable just below T_N, only simple commensurate structures with propagation vectors $\mathbf{Q}=0$, $\frac{1}{2}$, or $\frac{1}{4}$ can be observed at low temperature, leading to the possible occurrence of "devil's staircase" and "chaotic" states as a function of the temperature.[7–9] Using the same mean-field approach, Mashiyama found a finite number of commensurate phases at 0 K due to effectively long-range interactions.[10] More recently, biquadratic exchange has also been introduced in the ANNNI model to account for the sequence of incommensurate and commensurate states observed in UNi_2Si_2 when temperature is decreased.[11] An oversimplified so-called "incommensurate exchange field" model was proposed in 1988 by Date[12] to understand qualitatively the very complex magnetic phase diagram of CeSb. In this model, the spins are immersed in a phenomenological incommensurate exchange field. Although a lot of new features are qualitatively explained within both models, some limitations still remain, due to the restricted starting hypothesis. The more recent model developed by Iwata[13] to quantitatively account for the phase diagram of $PrCo_2Si_2$ represents a more realistic approach in which the complete variation of the Fourier transform of the exchange interactions

$J(\mathbf{q})$ along one direction of the Brillouin zone is taken into account.

In the present paper, we present a more general description of magnetic frustrated systems within the mean-field approximation. Although in some cases they can have some effect,[11] magnetic fluctuations are not taken into account. This approach is used to derive some features characteristic of anisotropic systems with frustrated interactions. Although these characteristics have been quoted here and there for some particular cases, we want to stress their general aspects. In particular, the effect of an external magnetic field has been rarely considered[14] and will be emphasized here. We then give examples of the increasing number of experimental systems which supports our conclusions.

The aim of the present paper is first to explain that, in the case of *axial anisotropy* systems, an incommensurate or long-period commensurate modulated structure occurring at T_N is *generally* unstable at 0 K and *must* exhibit a transition toward a structure with a shorter period. In this process, the role of higher-order harmonics in the Fourier expansion of the magnetic moments appears to be crucial. Secondly, we will show that, in these conditions, at 0 K, the magnetic field lowers the free energy of the incommensurate phases more rapidly than that of the simple commensurate ones, resulting in a *resurgence* of the high-temperature magnetic periodicity above a critical field. For that purpose, interionic magnetic interactions within the mean-field approximation will be shown to be the only ingredients required as soon as higher-order harmonics are correctly taken into account, the magnetocrystalline anisotropy being there only to force the magnetic moments to remain in a given direction. The calculations will be performed by using a self-consistent periodic-field (PF) model which has been successfully applied recently to describe the magnetic properties of several modulated systems, e.g., specific heat, magnetization processes, magnetic susceptibility, phase diagrams, etc.[15–17]

II. THE SELF-CONSISTENT PERIODIC-FIELD MODEL

The periodic-field (PF) model is based on an N-site Hamiltonian, N being the number of magnetic ions over one period of the modulated structure. In fact, a strictly incommensurate structure cannot be rigorously described, but one can expect to approach as close as possible to this limit by considering N large enough. On the other hand, the commensurate case is described by a propagation vector $\mathbf{Q}$ being a rational fraction of a reciprocal lattice vector $\mathbf{K}$, i.e., $\mathbf{Q}=(p/N)\mathbf{K}$ or $Q=p/N$ in reduced units: if the sequence of the magnetic moments along $\mathbf{Q}$ is considered [see Eq. (3) below], the structure can be reduced to a linear chain which includes only N independent magnetic moments. The PF model has been widely developed elsewhere,[15,16] and only some features are recalled below. The N-site Hamiltonian is written as

$$\mathcal{H}=\sum_{i=1}^{N}\mathcal{H}_{\mathrm{CEF}}(i)+\sum_{i=1}^{N}\mathcal{H}_Z(i)+\sum_{i=1}^{N}\mathcal{H}_B(i)+E_B \ . \quad (1)$$

In this expression, the first term is the crystalline electric-field (CEF) coupling from which the anisotropy originates. This term has generally two effects: (i) it may provide a preferential (easy) direction for the magnetic moments, leading to the occurrence of an amplitude modulated structure at T_N instead of a helical one, the latter being possible only in the case of a weak or an easy-plane anisotropy; (ii) by mixing the $4f$ wave functions, the CEF term raises the $(2J+1)$ degeneracy of the ground-state multiplet then may produce either a nonmagnetic or a magnetic level as the ground state—the case with a nonmagnetic ground state has been previously developed for $PrNi_2Si_2$.[16] In the following, only a magnetic ground state will be considered.

The second term $\mathcal{H}_Z$ in Eq. (1) is the Zeeman coupling $-\mathbf{H}\cdot\mathbf{M}(i)$ between the $4f$ magnetic moment $\mathbf{M}(i)=-g_J\mu_B\mathbf{J}(i)$ at site i and the external magnetic field $\mathbf{H}$. The third term $\mathcal{H}_B$ is the isotropic bilinear interaction $-\mathbf{H}_{\mathrm{ex}}(i)\cdot\mathbf{M}(i)$ written in the mean-field approximation as a function of the effective exchange field acting on the ith site:

$$\mathbf{H}_{\mathrm{ex}}(i)=(g_J\mu_B)^{-2}\sum_{j\neq i}J(ij)\langle\mathbf{M}(j)\rangle = \sum_n \mathbf{H}_{n\mathbf{Q}}e^{in\mathbf{Q}\cdot\mathbf{R}_i} \ . \quad (2)$$

The second part of this equation arises from the periodicity of the modulated structure which leads to a Fourier expansion of the magnetic moments $\langle\mathbf{M}(j)\rangle$:

$$\langle\mathbf{M}(j)\rangle=\sum_n \mathbf{M}_{n\mathbf{Q}}e^{in\mathbf{Q}\mathbf{R}_j} \ , \quad (3)$$

which defines the basic propagation vector $\mathbf{Q}$ of the magnetic structure. Therefore, it follows that the exchange field is also periodic with the same periodicity as $\mathbf{M}$, the Fourier harmonics $\mathbf{H}_{n\mathbf{Q}}$ being related in a very simple way to the corresponding harmonics $\mathbf{M}_{n\mathbf{Q}}$ of the magnetic moments through the Fourier transform $J(\mathbf{q})$ of the interionic exchange interactions $J(ij)$:

$$\mathbf{H}_{n\mathbf{Q}}=(g_J\mu_B)^{-2}J(n\mathbf{Q})\mathbf{M}_{n\mathbf{Q}} \ . \quad (4)$$

The last term in Eq. (1) is a corrective energy term

$$E_B=\frac{1}{2}\sum_{i=1}^{N}\langle\mathbf{M}(i)\rangle\mathbf{H}_{\mathrm{ex}}(i) \ ,$$

necessary due to the mean-field treatment. The full Hamiltonian, Eq. (1), has been diagonalized in a *self-consistent* manner for the N ions of one magnetic period, for any field and temperature value, the Fourier coefficients $\mathbf{M}_{n\mathbf{Q}}$ after a diagonalization being reinjected into the initial Hamiltonian through Eq. (4). It is then possible to evaluate all the magnetic or thermodynamical quantities needed, such as the magnetization or the free energy $F=-k_BT\ln(Z)$, where Z is the partition function, by averaging the values calculated for each ion over one period.[15,16]

III. TEMPERATURE DEPENDENCE OF THE FREE ENERGY

In a first step, the temperature variation of the free energy has been calculated for several commensurate mag-

netic structures having a periodicity varying from $N=2$ sites (simple antiferromagnet) to $N=50$ sites (close to a strictly incommensurate structure), and for various sets of $J(n\mathbf{Q})$'s, in order to simulate several cases of real systems. It can be noted that p has been taken as unity in the expression of $\mathbf{Q}$, i.e., $\mathbf{Q}=(1/N)\mathbf{K}$, because any other value of p leads to identical results for both the free energy and the net magnetization; the only difference is the sequence of the magnetic moments themselves along $\mathbf{Q}$, since multiplying $\mathbf{Q}$ by p is equivalent to multiply $\mathbf{R}_j$ by p in Eq. (3). On the other hand, and as in Ref. 15, all the calculations have been performed for a degenerated $J=\frac{7}{2}$ multiplet (and $g_J=2$), because considering any other value of J and nonzero CEF coupling leads to the *same qualitative* results, in as far as the ground state is *magnetic*. The only differences would be the absolute values of the free energies and magnetizations. Finally, the principal exchange coefficient $J(\mathbf{Q})$ has been taken as unity: indeed, only the relative magnitudes of the other harmonics $J(n\mathbf{Q})$'s (with $n\neq 1$) compared to $J(\mathbf{Q})$ are significant in the present results. Among all these harmonics, the Nth one plays a special role because it corresponds to the paramagnetic exchange coefficient $J(0)$; it has been systematically included and also kept constant [$J(0)=J(N\mathbf{Q})=-0.5$].

The main temperature variations of the free energy F in zero field are shown in Fig. 1 for various situations and allow one to clearly understand how the free energy depends on the periodicity and on higher-order harmonics. First, the overall variations up to the paramagnetic phase are presented for the extreme cases, i.e., for a simple antiferromagnetic ($N=2$) and for a quasi-incommensurate structure ($N=50$) for different sets of $J(n\mathbf{Q})$'s [see Fig. 1(a)]. The first curve ($N=2$) is universal [$F(T=0)=-1.167$ in reduced units] and depends only on J (and g_J); its deviation from the linear paramagnetic section starts from the ordering temperature T_N, the latter being defined below [Eq. (5)]. For this simple commensurate situation, considering higher-order harmonics is meaningless because they all are equivalent to the basic harmonic in the reciprocal space, and the curve does not depend on $J(0)$ either. It can be mentioned that this curve is also identical to that corresponding to a ferromagnetic structure with the appropriate exchange coupling, i.e., $J(0)=1$. The other curves are systematically all above the first one, and their $T=0$ limit directly depends on the relative magnitudes of the different $J(n\mathbf{Q})$'s [e.g., $F(0)=-0.947$ for $J(3Q)=0$, very close to the incommensurate limit -0.946]. This is understandable because in a long-period magnetic structure, even at $T=0$ where the full antiphase state is achieved, the variation of the exchange field keeps a certain modulation through Eq. (4) so that some sites experience an effective exchange field close to zero: the net averaged free energy is conse-

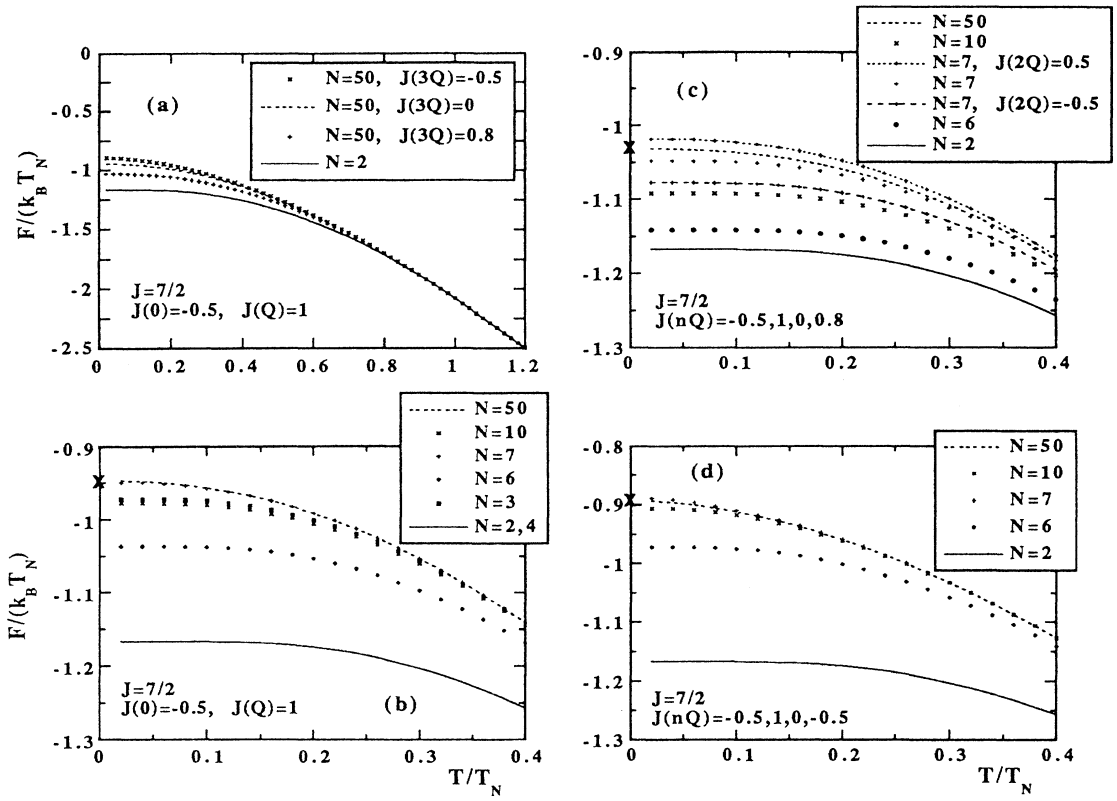

FIG. 1. Temperature dependence of the free energy for different sets of exchange coupling coefficients $J(n\mathbf{Q})$ (in reduced units); N is the number of magnetic sites over one period; in (c) and (d), the $N=2$ curve is drawn only for comparison, and the successive $J(n\mathbf{Q})$ values correspond to $n=0$, 1, 2, and 3; in (b)–(d), the cross indicates the limit of the strictly incommensurate case.

quently reduced in magnitude.

The other parts of Fig. 1 are devoted to the low-temperature variations of the free energies for $N=2$, 50, and several intermediate periodicities. In a general way, the values of N between the two extreme cases of 2 and 50 lead to intermediate curves, at least for the even values [see Fig. 1(b)]. The variations for odd values of N should also be inserted regularly among the others; however, they are shifted upward by the *negative* value of $J(0)$. Similarly, the second-order harmonic $J(2\mathbf{Q})$ directly influences the 0 K position of the odd-N curves [see $N=7$ in Fig. 1(c).] This emphasizes the different behavior of the even and odd parity of the magnetic periodicity: for *compensated* long-period structures (N even), the proportion of *up* and *down* moments is identical and only odd harmonics are involved in the Fourier expansion of the magnetic modulation (in zero magnetic field). It follows that only the odd order exchange coefficients $J[(2p+1)\mathbf{Q}]$ affect the temperature variation of the free energy. Oppositely, the *uncompensated* structures (N odd) develop, at low temperature, a spontaneous ferromagnetic component arising from the difference between *up* and *down* moments in the antiphase state: all the harmonics $J(n\mathbf{Q})$ (including $n=0$) are then involved in the free energy variation. It turns out that a periodicity of four sites gives rise to the same free energy variation as the case $N=2$, although it is associated to a sinusoidal structure at T_N evolving toward an antiphase structure at 0 K (sequence *up-up-down-down).* This is explained by the number of independent harmonics $J(n\mathbf{Q})$'s to be taken into account in the description of the structure. Due to the finite periodicity, the Fourier expansion must be truncated to at most N terms so that, in zero field, a single term then a single coefficient $J(\mathbf{Q})$ is concerned in the cases $N=1$, 2, and 4 (the effect of the field will be different, see below).

According to the magnitude of the higher-order harmonics, the free energy curves are more or less well separated, and they range from near the $N=2$ curve to more distant positions [compare, for example, Figs. 1(c) and 1(d)]. Note that the $N=50$ curve approaches very closely (within $\sim 0.2\%$) the incommensurate limit $F_{\text{inc}}(0)$ at $T=0$ [see Eq. (8) below and the crosses in Fig. 1], so that it can be reasonably considered as the incommensurate limit as far as the free energy is concerned. The various curves drawn in Fig. 1 show then a representative sampling of the free-energy variations for the different magnetic periodicities in the presence of various exchange couplings. The main conclusion of these calculations is that, for a given set of exchange coefficients $J(n\mathbf{Q})$'s, the shorter the periodicity, the lower are the free-energy curves at low temperature: this is because, *on average,* the magnitude of the local exchange field on all sites over one magnetic period is larger in such a case.

By applying a perturbation theory for small $M_{n\mathbf{Q}}$'s values,[16] it can be shown that the critical temperature T_c for a magnetic ordering having the propagation vector $\mathbf{Q}$ is defined by

$$(g_J\mu_B)^{-2}J(\mathbf{Q})\chi_0(T_c)=1 , \tag{5}$$

where $\chi_0(T)$ is the first-order magnetic susceptibility without exchange. As a consequence, the true ordering temperature T_N for real systems is the largest of all T_c's and corresponds to the periodicity for which $J(\mathbf{Q})$ is *maximum.* Obviously, the position of this maximum closely depends on the relative values of the successive $J_1, J_2, \ldots$ interionic coupling constants. In the vicinity of T_N, the free energy F can be expanded in powers of (T_N-T) in the same way as the internal energy and the specific heat (see Ref. 16):

$$F(T)=F_0(T_N)+(T-T_N)\frac{dF_0}{dT} + B(T_N-T)^2[\chi_0'(T_N)]^2/\chi_0^{(3)}(T_N) , \tag{6}$$

where $B=\frac{1}{6}$ or $\frac{1}{4}$ for an amplitude modulated (AM) or an equal moment (EM) structure, respectively, the latter corresponding to all the simple commensurate magnetic structures, i.e., ferromagnetic ($\mathbf{Q}=0$), simple antiferromagnetic ($\mathbf{Q}=\frac{1}{2}\mathbf{K}$) or $\mathbf{Q}=\frac{1}{4}\mathbf{K}$ (see above for the case $N=4$). $F_0(T)$ is the free energy without magnetic interactions; it depends only on the crystal field [$F_0=-k_BT\ln(2J+1)$ for a degenerated J multiplet]. $\chi_0^{(3)}(T)$ is the third-order magnetic susceptibility without exchange,[18] i.e., the initial curvature of the CEF magnetization curve, which is usually negative. As shown in Eqs. (6), the curvature of the free energy at T_N does not depend on the periodicity, except as far as the above distinction between AM and EM systems is concerned, the curvature always being the strongest for these latter, in agreement with the curves described above.

As a matter of fact, it can be shown that the propagation vector $\mathbf{Q}$ for which $J(\mathbf{Q})$ is maximum generally *does not* minimize the free energy at 0 K, resulting in a change of the propagation vector toward another value associated with a shorter periodicity. At 0 K, and for a strictly incommensurate periodicity, the free energy can be written as[15]

$$F_{\text{inc}}(0)=F_0(0)-\frac{1}{2}(g_J\mu_B)^{-2}\sum_n J(n\mathbf{Q})|\mathbf{M}_{n\mathbf{Q}}|^2 , \tag{7}$$

where $F_0(0)$ includes the CEF contribution and the second term represents only the exchange coupling term. For an antiphase-type moment configuration, all the successive $M_{n\mathbf{Q}}$'s ($n>1$) are related to each other, so that Eq. (7) can be rewritten as[16]

$$F_{\text{inc}}(0)=F_0-\frac{4}{\pi^2}(g_J\mu_B)^{-2}|\mathbf{M}_0|^2 \times[J(\mathbf{Q})+\tfrac{1}{9}J(3\mathbf{Q})+\tfrac{1}{25}J(5\mathbf{Q})+\cdots] , \tag{8}$$

where M_0 is the magnitude of the magnetic moment at 0 K. It is obvious that, if $dJ(\mathbf{q})/d|\mathbf{q}|$ vanishes at the maximum of $J(\mathbf{Q})$, the same will not generally be true for the full expression between brackets in Eq. (8) at 0 K. There *must* be another propagation vector $\mathbf{Q}_0$, strictly incommensurate or not, which maximizes this expression. This is a direct consequence of including the higher-order harmonics $J(3\mathbf{Q}), J(5\mathbf{Q}), \ldots$ in the free energy expression at 0 K. In addition, it should be mentioned that the expression of $F(0)$ for a commensurate periodicity is different

from Eq. (8) because the summation must be truncated (see above). Finding this $\mathbf{Q}_0$ vector requires the knowledge of the actual shape of $J(\mathbf{q})$ in the entire first Brillouin zone, and appears to be a formidable task. Nevertheless, as shown by the temperature variation of the free energies (see Fig. 1), one can expect that $\mathbf{Q}_0$ will very likely correspond to a short-period commensurate vector. It is worth noting that $J(\mathbf{Q}_0)$ is always smaller than $J(\mathbf{Q})$, therefore, at 0 K, the *loss* of energy due to the first harmonic $J(\mathbf{Q}_0)$ must be overcompensated by a larger *gain* of energy due to all the higher-order harmonics.

IV. FIELD DEPENDENCE OF THE FREE ENERGY

The second part of this study is devoted to the external field dependence of the free energy. Calculations have been performed in the same conditions as above, i.e., for the same set of exchange parameters and periodicities, using reduced units. Note that the magnetic field has been renormalized by

$$H_0=\frac{3k_BT_N}{g_J\mu_B(J+1)} . \tag{9}$$

Figure 2 shows the field variations when only $J(0)$ and $J(\mathbf{Q})$ are considered. The case $N=2$ is the simplest one [Fig. 2(a)]; a single first-order transition for a critical field $H_c/H_0=0.746$ separates the simple antiferromagnetic state $(1\bar{1})$, i.e., a sequence *up-down,* from the *induced ferromagnetic* (IF) state (20), i.e., *up-up:* during the first part of this process, the magnetization is zero and the free energy constant, while during the second part, the magnetization reaches the saturated value $M_0=-g_J\mu_BJ$, corresponding to the slope of the linear variation of the free energy. Note that the notation $(m\bar{n})$ will be used to describe the sequence of m moments *up* followed by n moments *down.* For a periodicity of four sites [$N=4$, Fig. 2(a)], the same two states as for $N=2$ are also present, i.e., the sequences $(2\bar{2})$ and (40), but there is an additional intermediate configuration $(3\bar{1})$ stabilized between $H_{c1}/H_0=0.625$ and $H_{c2}/H_0=0.867$, corresponding to a net magnetization of one half of the saturated value.

As the period (i.e., N) increases, the number of intermediate configurations grows, as shown on the curve for $N=10$ [Fig. 2(c)] where some sequences however, e.g., $(8\bar{2})$, are never the ground state for any field, so that the magnetization jumps at $H_c/H_0=0.806$ from $\frac{4}{10}M_0$ [sequence $(7\bar{3})$] to M_0 (IF state). For $N=50$, the incommensurate limit is approached, and the free energy curve exhibits a curvature increasing monotonically until it crosses the IF variation at $H_c/H_0=0.792$ [Fig. 2(d)]. At the incommensurate limit, the magnetization process no longer presents any steps but the magnetization increases continuously up to the field transition where one single step occurs. In the case of odd periodicity [e.g, $N=7$, Fig. 2(b)], the initial nonzero slope of the free energy variation is consistent with the existence of a spontaneous ferromagnetic moment arising from the lack of compen-

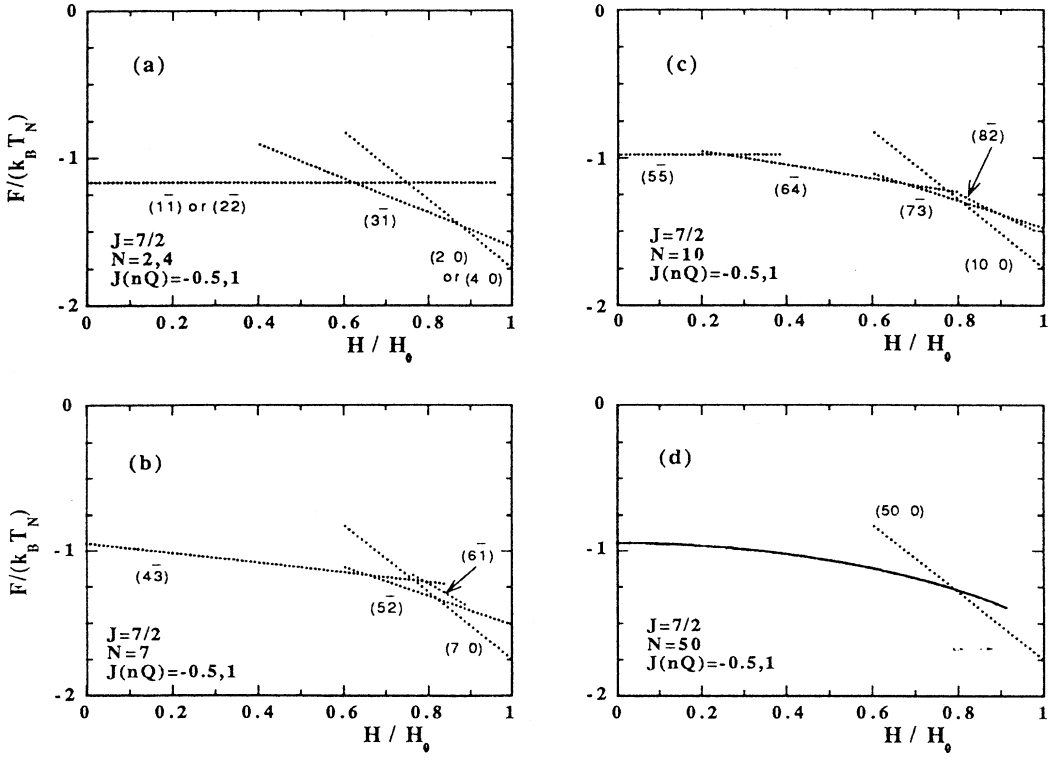

FIG. 2. Field dependence of the free energy for $J(0)=-0.5$ and $J(\mathbf{Q})=1$, and for different periodicities (in reduced units); N is the number of sites over one period; labels $(m\bar{n})$ refer to a (m *up*–n *down*) sequence for the magnetic moments.

sation in the $(4\bar{3})$ magnetic sequence.

For all curves, the starting point at $H=0$ depends on the magnetic periodicity as explained above for the $T=0$ limit. However, if we compare the two extreme situations, i.e., $N=2$ and 50, it turns out that both field variations intersect for $H_c/H_0=0.665$, considering the same set of exchange parameters. This critical field should be reduced according to the actual magnitude of $J(\mathbf{Q})$ for the vector corresponding to the simple antiferromagnet, if the incommensurate structure is considered as the most stable at T_N. The main conclusion is that the *resurgence* of the incommensurate or long-period commensurate structure in high field appears as quite probable, because its free energy decreases more rapidly in increasing field than that of commensurate structures with a shorter period. This is related to the fact that, in long-period structures, a larger number of magnetic moments "see" a reduced exchange field and can then flip in a smaller opposite external field.

The two other figures 3 and 4 show the effects of higher-order exchange coefficients on the free-energy variations. According to their sign, they shift the curves for the different configurations up or down, so that some forbidden states may become stable in a limited field range as, for example, the sequence $(8\bar{2})$ with $N=10$ for a positive $J(3\mathbf{Q})$ [see Fig. 3(b)]. More surprisingly, new exotic sequences may be stabilized, such as the sequence $(4\bar{1}1\bar{1})$ with $N=7$ [Fig. 3(a)], emphasizing a strongly distorted shape for the exchange field over one period, due to the presence of a large third harmonic $J(3\mathbf{Q})$. In the same way, the $N=100$ curve reveals the appearance of an intermediate configuration for a positive $J(3\mathbf{Q})$ value, leading to an intermediate step and two large discontinuous jumps in the magnetization process. Similarly, including a second rank exchange coefficient $J(2\mathbf{Q})$ produces new possible configurations, as shown by the sequence $(6\bar{1}2\bar{1})$ for $N=10$ [see Fig. 4(b)]. All these curves underline the variety of possible situations which can be stabilized under an external field. Describing experimental systems requires the knowledge of the actual exchange coupling, i.e., $J(\mathbf{q})$. This exchange coupling can be determined either from inelastic neutron scattering on single crystal or from the fit of the right sequence of propagation vectors and magnetization as a function of field and temperature.

V. DISCUSSION

The above results are useful in that they give some very general features of the field-temperature phase diagrams of systems with *axial anisotropy,* taking into account the real variation of $J(\mathbf{q})$. As quoted above, the propagation vector $\mathbf{Q}_N$ of the magnetic structure just below T_N is that for which $J(\mathbf{q})$ is maximum. Due to the long period and oscillatory character of the exchange interactions, the associated magnetic periodicity can also have any value, incommensurate or long- or short-period commensurate, with the lattice. As we will see later, the former situation is observed for a lot of compounds. In most cases at lower temperature the value of $\mathbf{Q}_N$ does not minimize the

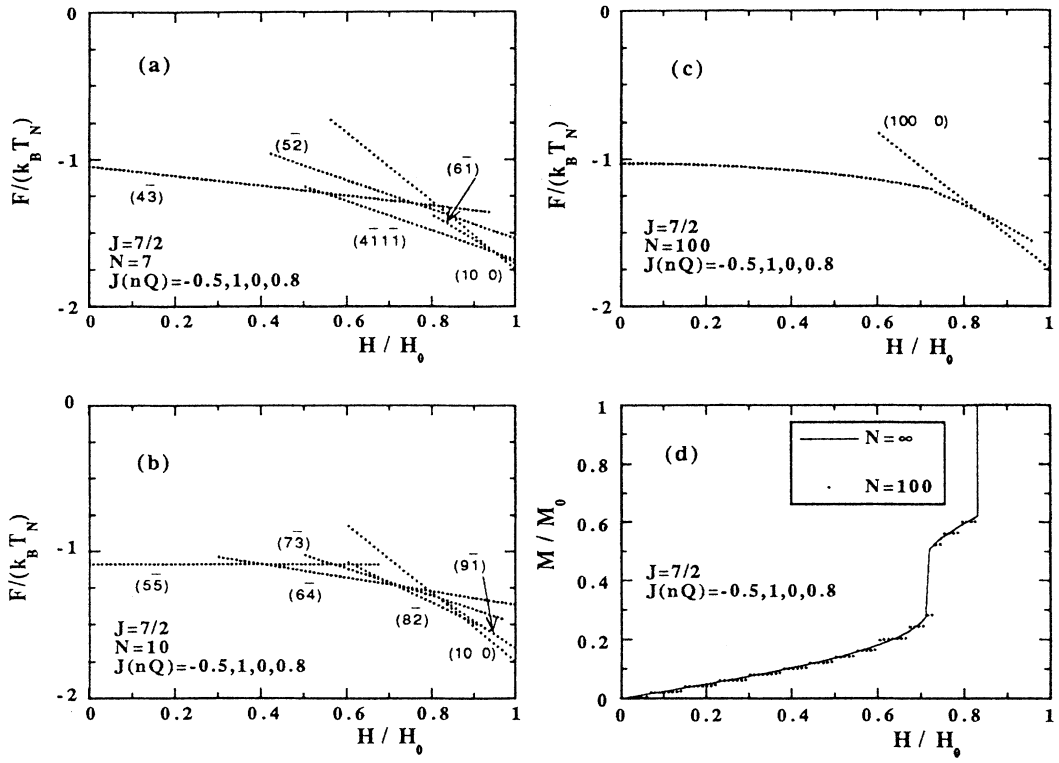

FIG. 3. As in Fig. 2, for the indicated set of exchange coefficients $J(n\mathbf{Q})$ $(n=0,1,2,3)$; (d) represents the magnetization curve associated with the free energy variation of (c).

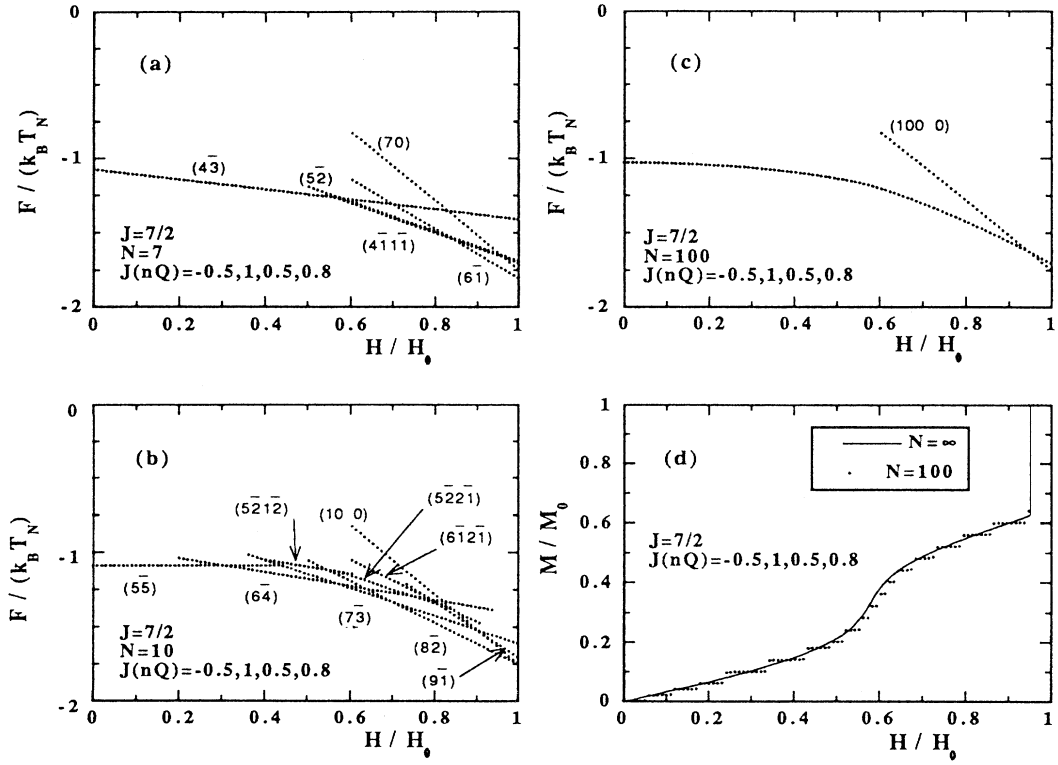

FIG. 4. As in Fig. 3, but for another set of exchange coefficients $J(n\mathbf{Q})$.

free energy, in particular, at $T=0$ K. As shown by the curves in Fig. 1, commensurate magnetic periodicities with short-period $\mathbf{Q}_{sp}$ are always favored as long as $J(\mathbf{Q}_{sp})$ and higher-order harmonics are not too small compared to $J(\mathbf{Q}_N)$ and higher-order harmonics of the high-temperature state. The most favored states at 0 K are the simple commensurate states with $N=1$ (ferro), 2, or 4, i.e., $Q_0=0$, $\frac{1}{2}$, or $\frac{1}{4}$ in reduced units. Obviously among these three states the system will choose that which has the largest associated $J(\mathbf{q})$ value. Let this value be J_0; in the case of $N=50$, which is close to the incommensurate limit, and ignoring the higher-order $J(n\mathbf{Q}_N)$'s $(n>1)$, calculation shows that if the ratio $J(\mathbf{Q}_N)/J_0$ is not larger than 1.23 the simple commensurate state is stabilized at low temperature. Such a situation is the most probable and indeed we will see below that the majority of experimental systems enters this category. Free energies calculated (Fig. 1) for $Q=\frac{1}{50}$ with $J(3Q)=-0.5$ and 0.8 allow us to appreciate the effect of higher-order harmonics on the stability at 0 K of the simple commensurate state compared to the incommensurate one. We can then conclude that generally, within the framework of our assumptions, magnetic structures are *incommensurate* (or long-period commensurate) and *sine wave modulated* at T_N and transform toward a simple equal moments *commensurate* state below a given temperature T_t through a first-order transition. This is illustrated in Fig. 5 assuming that the maximum of $J(\mathbf{q})$ occurs for $Q=\frac{3}{10}$ and that $J(\frac{3}{10})=5.71$ K whereas $J(\frac{1}{2})=5.43$ K and $J(0)=-2.86$ K [instead of $Q=\frac{1}{10}$, which leads to the same energy, $Q=\frac{3}{10}$ has been chosen so that the values of $J(0)$, $J(\frac{3}{10})$, and $J(\frac{1}{2})$ correspond to a realistic variation of $J(\mathbf{q})$]. The state with the lowest energy is the long-period $(N=10)$ state between $T_N=10$ K and $T_t=7.4$ K, and becomes the $N=2$ state below this later temperature. Depending on the real variation of $J(\mathbf{q})$, intermediate states with intermediate propagation vectors can be stabilized. Furthermore, calculation shows that, except near T_N, a commensurate long-period state tends to be stabilized instead of a true

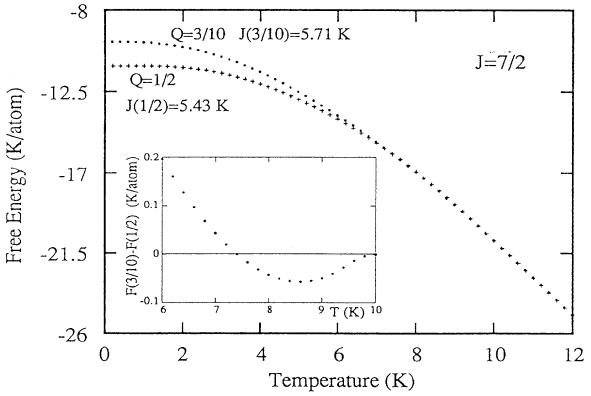

FIG. 5. Temperature dependence of the free energy for $N=2$ and 10 but with different associated $J(\mathbf{q})$ values. The inset shows the energy difference of the two states between 6 and 10 K.

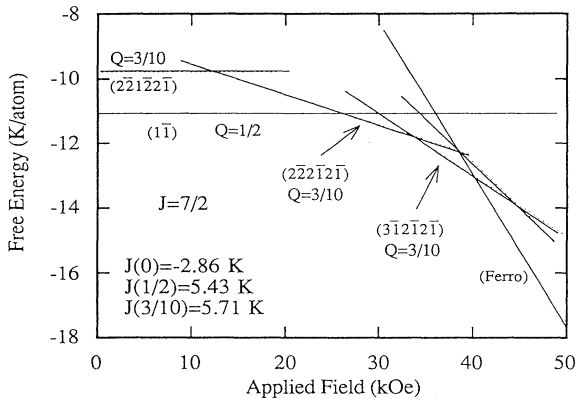

FIG. 6. Fields dependences of the free energy in the two situations of Fig. 5.

incommensurate state. Figure 6 shows field effects on the low-temperature magnetic structure of the above example. This figure demonstrates an important result: the long-period structure, corresponding to the maximum value of $J(\mathbf{q})$, is restored before the IF state is stabilized.

In Table I, we have reported the magnetic structures of a large number of rare-earth based intermetallic compounds in which the large axial magnetocrystalline anisotropy imposes collinear magnetic structures. This table clearly supports the thermal characteristics set out above. All these compounds have *incommensurate modulated* structures at T_N and transform toward *equal moment commensurate* states at low temperature. Note that almost all these compounds are simple commensurate of the type $N=1$, 2, or 4 at low temperature. The case $Q=\frac{1}{4}$ is especially scarce and appears only once in our list ($TbCo_2B_2$). In our examples only two compounds (HoAlGa and $PrGa_2$) are not simple commensurate at low temperature, although, for the first compound, the extremity of the propagation vector $(\frac{1}{3},\frac{1}{3},\frac{1}{2})$ falls on a high-symmetry point of the Brillouin zone. In some compounds (e.g., $PrCo_2Si_2$ and $NdCo_2Si_2$) intermediate states with intermediate propagation vectors are observed. Moreover, in some cases (e.g., $TbAu_2$, $TbZn_2$, and ErSi) the propagation vector seems to continuously change with temperature down to a given temperature below which it locks on to a simple commensurate value whereas in the majority of compounds the propagation vectors are temperature independent over a large temperature range.

The number of studies devoted to the determination of the field-induced magnetic structure is quite limited. Among the compounds listed in the table only $PrCo_2Si_2$ (Ref. 42), $TbNi_2Si_2$ (Ref. 43), and HoAlGa (Ref. 44) have been studied by neutron diffraction under the magnetic field on a single crystal. In these three compounds, in the low-temperature metamagnetic process, the high-temperature propagation vectors are recovered. Note that in the two latter compounds this means that an incommensurate phase is induced by the field; a property which at first sight can seem unexpected. In $PrCo_2Si_2$, which exhibits three steps in the low-temperature magnetization process, the first metamagnetic step stabilizes the $\frac{25}{27}$ propagation vector and the second step stabilizes the $\frac{7}{9}$

TABLE I. Propagation vectors of many rare-earth–based intermetallic compounds in which crystal-field effects impose collinear magnetic structures.

Compound		Symmetry	Sequence of Q (in reduced units) and transition temperatures		Ref.
$PrFe_2Ge_2$	Tetragonal	$(0,0,\frac{1}{2})_{9\ K}$—		$(0,0,0.476)_{13\ K}$	19
$PrCo_2Si_2$		$(0,0,1)_{9\ K}$—	$(0,0,\frac{25}{27})_{17\ K}$—	$(0,0,\frac{7}{9})_{30\ K}$	20
$NdCo_2Si_2$		$(0,0,1)_{15\ K}$—	$(0,0,\frac{13}{14})_{24\ K}$—	$(0,0,\frac{11}{14})_{32\ K}$	21
$NdCo_2Ge_2$		$(0,0,1)_{12\ K}$—		$(0,0,0.739)_{28\ K}$	22
$NdRu_2Si_2$		$(0,0,0)_{10\ K}$—		$(0.13,0.13,0)_{26\ K}$	23
$NdRu_2Ge_2$		$(0,0,0)_{10\ K}$—		$(0.12,0.12,0)_{17\ K}$	24
$TbNi_2Si_2$		$(\frac{1}{2},\frac{1}{2},0)_{8.5\ K}$—		$(0.574,0.426,0)_{14\ K}$	25
$TbCo_2B_2$		$(\frac{1}{4},\frac{1}{4},0)_{10\ K}$—		$(0.244,0.244,0)_{19\ K}$	26,27
$NdIn_3$	Cubic	$(1,0,0)_{4.6\ K}$—	$(1,0,0.02)_{5.1\ K}$—	$(1,0,0.04)_{6\ K}$	28
Ce_4Bi_3		$(0,0,0)_{3.3\ K}$—		$(0,0,0.506)_{4.4\ K}$	29
$DyGa_2$	Hexagonal	$(\frac{1}{2},\frac{1}{2},0)_{6.1\ K}$—		$(0.433,0.433,0)_{11.2\ K}$	30
$HoGa_2$		$(\frac{1}{2},\frac{1}{2},0)_{6.5\ K}$—		$(0.439,0.439,0)_{7.6\ K}$	31
HoAlGa		$(\frac{1}{3},\frac{1}{3},\frac{1}{2})_{18.5\ K}$—		$(\frac{1}{3},\frac{1}{3},0.481)_{32\ K}$	32
$CeGa_2$		$(0,0,0)_{8.5\ K}$—	$(0.08-\tau,2\tau,0)_{10.4\ K}$—	$(0.14,0.14,0)_{11\ K}$	33
$PrGa_2$		$(\frac{4}{27},\frac{4}{27},0)_{3.2\ K}$—		$(0.148,0.148,0.023)_{7.3\ K}$	34
$ErAu_2$	Tetragonal	$(1,0,0)_{4\ K}$—		$(0.801,0,0)_{6.7\ K}$	35
$HoAu_2$		$(1,0,0)_{7.8\ K}$—		$(0.814,0,0)_{9.2\ K}$	36
$ErAg_2$		$(1,0,0)_{3.5\ K}$—		$(0.783,0,0)_{5.2\ K}$	37
$TbAu_2$		$(1,0,0)_{42.5\ K}$—		$(\tau,0,0)$ with $0.833<\tau<0.843_{55\ K}$	38
$DyAu_2$		$(1,0,0)_{33.8\ K}$—		$(0.826,0,0)_{25.5\ K}$	39
$DyAg_2$		$(1,0,0)_{9.5\ K}$—		$(0.855,0,0)_{15\ K}$	39
$TbZn_2$	Orthorhombic	$(0,0,\frac{1}{2})_{60\ K}$—		$(0,0,\tau)$ with $0.394<\tau<0.438_{75\ K}$	40
ErSi		$(\frac{1}{2},0,\frac{1}{2})_{5.75\ K}$—		$(\tau,0,\tau')$ with $0.460\leq\tau\leq0.5$ and $0.5\leq\tau'\leq0.512_{11.5\ K}$	41

vector whereas a third transition is necessary to reach the IF state.[42] These two vectors are precisely those which are successively observed when temperature is increased (see Table I). Although no reliable crystal-field parameters have been determined, it is in this compound that the deepest analysis in terms of exchange interactions has been performed.[13] In particular, a $J(\mathbf{q})$ variation has been determined which quantitatively accounts for the H-T phase diagram.

We did not mention the well-known CeSb compound because its very complex phase diagram, with many different magnetic structures,[45] cannot be accommodated in Table I. Although this system exhibits some unique properties (in particular, the existence of paramagnetic moments below T_N) and although other interpretations of its magnetic phase diagram have been proposed we are forced to observe that it presents the behavior characteristic of our model, i.e., (i) a devil's staircase is observed from the high-temperature propagation vector $Q=\frac{2}{3}$ to the low-temperature simple commensurate vector $Q=\frac{1}{2}$ through five intermediate phases with intermediate propagation vectors and (ii) during the low-temperature magnetization process one observes a recovery of some of the high-temperature propagation vectors.

In conclusion, a realistic mean-field model allowed us to account for the origin of the main characteristics of the complex magnetic phase diagrams observed in many rare-earth based intermetallics compounds, in which the magnetocrystalline anisotropy imposes *collinear* magnetic structures. These are (i) just below the Néel temperature the magnetic structure is modulated and *incommensurate or long-period commensurate,* (ii) when the crystal-field ground state is magnetic, at low temperature the magnetic structure becomes an equal moment and *simple commensurate,* and (iii) during the low-temperature metamagnetic process a *resurgence* of the high-temperature incommensurate or commensurate propagation vector(s) is induced by the field before the IF is reached. Note that in Spin-Peierls systems it has been found that, at low temperature, an applied magnetic field could induce a simple commensurate to incommensurate phase transition of the lattice distortion.[46] It is important to stress that *all these features arise from exchange interactions alone,* the role of crystal field being to impose the moment direction and to contribute to the exact position of the boundaries of the H-T phase diagram, in particular, the exact values of T_N, the T_t's, and the critical fields.

[1]For a review, see P. Bak, Rep. Prog. Phys. **45**, 587 (1982) and references therein.

[2]A. Szytula and J. Leciejewicz, *Handbook on the Physics and Chemistry of Rare Earths,* Vol. 12, edited by K. A. Gschneidner, Jr. and L. Eyring (Elsevier, New York, 1989), p. 132; A. Szytula, J. Alloys Compounds **178**, 1 (1992)..

[3]D. Gignoux and D. Schmitt, J. Magn. Magn. Mater. **100**, 99 (1991).

[4]P. Bak and J. von Boehm, Phys. Rev. B **21**, 5297 (1980).

[5]M. E. Fisher and W. Selke, Phys. Rev. Lett. **44**, 1502 (1980).

[6]W. Selke and P. M. Duxbury, Z. Phys. B **57**, 49 (1984).

[7]M. H. Jensen and P. Bak, Phys. Rev. B **27**, 6853 (1983).

[8]K. Nakanashi and H. Shiba, J. Phys. Soc. Jpn. **51**, 2089 (1982).

[9]K. Nakanashi, J. Phys. Soc. Jpn. **52**, 2449 (1983).

[10]H. Mashiyama, J. Phys. C **16**, 187 (1983).

[11]A. Mailhot, M. L. Plumer, A. Caillé, and P. Azaria, Phys. Rev. B **45**, 10 399 (1992).

[12]M. Date, J. Phys. Soc. Jpn. **57**, 3682 (1988).

[13]N. Iwata, J. Magn. Magn. Mater. **86**, 225 (1990).

[14]N. Ishimura, J. Phys. Soc. Jpn. **54**, 4752 (1985).

[15]J. A. Blanco, D. Gignoux, and D. Schmitt, Phys. Rev. B **43**, 13 145 (1991).

[16]J. A. Blanco, D. Schmitt, and J. C. Gomez-Sal, J. Magn. Magn. Mater. **116**, 128 (1992).

[17]A. R. Ball, D. Gignoux, D. Schmitt, and F. Y. Zhang, Phys. Rev. B **47**, 11 887 (1993).

[18]P. Morin and D. Schmitt, in *Ferromagnetic Materials,* Vol. 5, edited by E. P. Wolfarth and K. H. J. Buschow (North-Holland, Amsterdam, 1990), Chap. 1.

[19]A. Szytula, A. Oles, and A. Perrin, J. Magn. Magn. Mater. **86**, 377 (1990).

[20]T. Shigeoka, N. Iwata, Y. Hashimoto, Y. Andoh, and H. Fujii, Physica B **156-157**, 741 (1989).

[21]T. Shigeoka, N. Iwata, Y. Hasimoto, Y. Andoh, and H. Fujii, J. Phys. **49**, C8-431 (1988).

[22]G. André, F. Bourée-Vigneron, A. Oles, and A. Szytula, J. Magn. Magn. Mater. **86**, 387 (1990).

[23]B. Chevalier, J. Etourneau, J. Hagenmuller, P. M. Quezel, and J. Rossat-Mignod, J. Less Commun. Met. **111**, 161 (1985).

[24]A. Szytula, A. Oles, M. Perrin, M. Slaski, W. Kwok, Z. Sungaila, and B. D. Dunlap, J. Magn. Magn. Mater. **69**, 305 (1987).

[25]J. M. Barandiaran, D. Gignoux, D. Schmitt, J. C. Gomez Sal, and J. Rodriguez Fernandez, J. Magn. Magn. Mater. **69**, 61 (1987).

[26]G. André, P. Thuéry, M. Pinot, A. Oles, and A. Szytula, Solid State Commun. **80**, 239 (1991).

[27]M. L. Plumer and A. Caillé, Phys. Rev. B **46**, 203 (1992).

[28]S. Mitsuda, P. M. Gehring, G. Shirane, K. Yoshizawa, and Y. Onuki, J. Phys. Soc. Jpn. **61**, 1469 (1992).

[29]J. A. Alonso, J. X. Boucherle, J. Rossat-Mignod, J. Schweizer, T. Suzuki, and T. Kasuya, J. Magn. Magn. Mater. **103**, 179 (1992).

[30]D. Gignoux, D. Schmitt, A. Takeuchi, and F. Y. Zhang, J. Magn. Magn. Mater. **97**, 15 (1991).

[31]D. Gignoux, D. Schmitt, and F. Y. Zhang (unpublished).

[32]D. Gignoux, D. Schmitt, A. Takeuchi, F. Y. Zhang, C. Rouchon, and E. Roudaut, J. Magn. Magn. Mater. **98**, 333 (1991).

[33]M. Jerjini, M. Bonnet, P. Burlet, G. Lapertot, J. Rossat-Mignod, J. Y. Henry, and D. Gignoux, J. Magn. Magn. Mater. **76-77**, 405 (1988).

[34]A. R. Ball, D. Gignoux, and D. Schmitt, Physica B **180-181**, 58 (1992).

[35]M. Atoji, J. Chem. Phys. **57**, 2407 (1972).

[36]M. Atoji, J. Chem. Phys. **57**, 2402 (1972).

[37]M. Atoji, J. Chem. Phys. **57**, 851 (1972).

[38]M. Atoji, J. Chem. Phys. **48**, 560 (1968).

[39]M. Atoji, J. Chem. Phys. **51**, 3877 (1969).
[40]D. Debray, M. Sougi, and P. Meriel, J. Chem. Phys. **56**, 4325 (1972).
[41]P. Thuéry, G. André, F. El Maziani, M. Clin, and P. Schobinger-Papamantellos, J. Magn. Magn. Mater. **109**, 197 (1992).
[42]H. Nojiri, M. Uchi, S. Watamura, M. Motokawa, H. Kawai, Y. Endoh, and T. Shigeoka, J. Phys. Soc. Jpn. **60**, 2380 (1991).
[43]J. A. Blanco, D. Gignoux, D. Schmitt, and C. Vettier, J. Magn. Magn. **97**, 4 (1991).
[44]A. R. Ball, D. Gignoux, D. Schmitt, F. Y. Zhang, and M. Reehuis, J. Magn. Magn. Mater. **110**, 343 (1992).
[45]J. Rossat-Mignod, P. Burlet, L. P. Regnault, and C. Vettier, J. Magn. Magn. Mater. **90-91**, 5 (1990).
[46]A. Kotani and I. Harada, J. Phys. Soc. Jpn. **49**, 535 (1980); I. Harada and A. Kotani, *ibid.* **51**, 1737 (1982).